J Ind Microbiol Biotechnol (2012) 39:843–850
DOI 10.1007/s10295-012-1092-2

BIOENERGY/BIOFUELS/BIOCHEMICALS

Photosynthetic accumulation of carbon storage compounds under CO_2 enrichment by the thermophilic cyanobacterium *Thermosynechococcus elongatus*

Jed O. Eberly · Roger L. Ely

Received: 7 September 2011 / Accepted: 18 January 2012 / Published online: 1 March 2012

Abstract The growth characteristics of *Thermosynechococcus elongatus* on elevated CO_2 were studied in a photobioreactor. Cultures were able to grow on up to 20% CO_2. The maximum productivity and CO_2 fixation rates were 0.09 ± 0.01 and 0.17 ± 0.01 mg ml^{-1} day^{-1}, respectively, for cultures grown on 20% CO_2. Three major carbon pools—lipids, polyhydroxybutyrates (PHBs), and glycogen—were measured. These carbon stores accounted for 50% of the total biomass carbon in cultures grown on atmospheric CO_2 (no supplemental CO_2), but only accounted for 30% of the total biomass carbon in cultures grown on 5–20% CO_2. Lipid content was approximately 20% (w/w) under all experimental conditions, while PHB content reached 14.5% (w/w) in cultures grown on atmospheric CO_2 and decreased to approximately 2.0% (w/w) at 5–20% CO_2. Glycogen levels did not vary significantly and remained about 1.4% (w/w) under all test conditions. The maximum amount of CO_2 sequestered over the course of the nine-day chemostat experiment was 1.15 g l^{-1} in cultures grown on 20% CO_2.

Introduction

The past decade has seen a renewed interest in biofuel and biomaterial research corresponding to declining petroleum reserves and the consequent rise in energy costs. Cyanobacteria are ideal organisms for producing biofuels and bioproducts because of their ability to utilize solar energy directly. Cyanobacteria also assimilate CO_2 and thus may also be an effective means of mitigating rising CO_2 levels while generating biofuels and other valuable bioproducts. Recent reviews have discussed the numerous advantages of combined CO_2 mitigation and biofuels production by microorganisms [2, 41, 42, 44]. This has driven recent efforts in utilizing cyanobacteria and algae for carbon sequestration at power plants and other industrial facilities that produce flue gas, which can contain up to 20% CO_2 [19]. The higher CO_2 concentrations found in industrial flue gas could contribute to improved growth rates, since the atmosphere contains only 0.03–0.06% CO_2 [44]. Cyanobacteria are also effective at removing nitrogen and phosphorus [28], and aid in metal ion depletion [44], which makes them suitable for wastewater treatment, thereby providing an additional benefit for industrial waste processing.

Using closed photobioreactors to culture cyanobacteria for CO_2 sequestration offers several advantages. First, increased concentrations of CO_2 can be fed to the cultures, leading to improved productivity. Second, water-use efficiency is greater since evaporation is minimized. Finally, environmental conditions can be carefully controlled, thus minimizing contamination.

There are several obstacles to efficient CO_2 sequestration by cyanobacteria. One key limitation in CO_2 utilization by photosynthetic microbes can be low mass transfer of gas-phase CO_2 into water in poorly mixed systems [11]. Even though gas-phase CO_2 levels may be relatively high, if the mass transfer of CO_2 is too low, the low availability of CO_2 in solution may limit culture growth. Another limitation on CO_2 sequestration and

J. O. Eberly · R. L. Ely
Department of Biological and Ecological Engineering, Oregon State University, 116 Gilmore Hall, Corvallis, OR 97331, USA

J. O. Eberly (✉)
Environmental Laboratory, CEERDC-EP-P, US Army Engineer Research and Development Center, 3909 Halls Ferry Road, Vicksburg, MS 39180, USA
e-mail: Jed.O.Eberly@usace.army.mil

biomass production is the elevated temperatures that can be encountered in bioreactors operated in direct sunlight. In a recent review, Mata et al. [29] reported that the effect of temperature on biomass production is an important factor that has not yet been sufficiently acknowledged in biomass production and renewable energy research. Part of this limitation is the temperature-dependent solubility of CO_2. As temperature increases, CO_2 solubility decreases, thus lowering the available CO_2. At 30°C, the physiological optima of many cyanobacteria, the Henry's law constant of CO_2 in water is 2.965×10^{-2} mol/l atm while at 50°C it decreases to 1.817×10^{-2} mol/l atm [10]. Temperatures in photobioreactors can reach 55°C on hot days [29], thus necessitating the use of cooling systems to maintain a constant temperature. Utilizing thermophilic organisms would minimize the amount of energy expended on cooling, thereby contributing to the overall efficiency of the system.

Cyanobacteria store carbon primarily as glycogen [23], while some species also accumulate large reserves of polyhydroxyalkanoates (PHAs) such as polyhydroxybutyrates (PHBs) [33, 43], all of which have potential uses for biofuels or biomaterials. Cyanobacteria can also be used as a source of biomass for gasification and pyrolysis for generating fuels [18]. In addition, cyanobacteria are a source of compounds such as acetylic acid, β-carotene, vitamin B, carotenoids, polyunsaturated fatty acids, lutein, and cyanophycin, which are of value in the health food, pigment, and pharmaceutical industries [15, 16, 26].

Thermophilic cyanobacteria represent a unique subset of phototrophs with characteristics that make them particularly amenable to industrial CO_2 sequestration. The higher optimal growth temperature lowers the likelihood of competing species and may enable them to grow in the high-temperature wastewater and flue gas streams emitted from industrial plants.

Thermosynechococcus elongatus is a unicellular, obligately autotrophic cyanobacterium that grows in hot springs at a temperature of 48–55°C [35]. The photosystems of *T. elongatus* have served as models for extensive structural studies due to their extraordinary stability [21, 27], but little is known about the metabolic pathways in this organism. This is due in part to the fact that it is an obligate autotroph and thus not amenable to the significant knockout mutations that are often needed to analyze metabolic pathways.

The aim of this study was to characterize the growth of *T. elongatus* on increasing levels of CO_2 and to determine the carbon uptake rates and maximum productivity in a bioreactor configuration. Accumulation of carbon storage compounds with biofuel and bioproduct potential was also examined.

Materials and methods

Culturing conditions

Thermosynechococcus elongatus BP-1 was cultured in BG-11 media [5] supplemented with TES-KOH at pH 7.8. Cell growth was monitored by measuring the optical density of the cultures at 730 nm, and chlorophyll concentrations were determined using methanol extraction followed by spectrophotometric measurement at 665 nm, with concentrations calculated by the method of Porra [38].

Bioreactor experiments

Bioreactor experiments were carried out in Applikon 3 l water-jacketed glass reactor vessels with a 2.7 l working volume, connected to Applikon ADI 1025 and 1035 Bioconsoles controlled by ADI 1010 and 1020 Biocontrollers (Applikon, Schiedam, Netherlands). Gas flow was controlled using the built-in rotameters. Cultures were grown at 50°C, pH 7.8 with a stir speed of 300 rpm. Higher stir speeds were avoided because they were detrimental to growth and contributed to foaming. Light was supplied from below at 180 μE m^{-2} s^{-1}. Reactors were bubbled with a mixture of sterile filtered air and CO_2 at a flow rate of 20 ml/min for an aeration rate of 0.0074 vvm. The reactors were well mixed, with a K_La of 4.07 min^{-1}, estimated according to the methods of van't Riet [39] and Gill et al. [14]. Cultures were grown under atmospheric, 5, 10, 20, and 30% CO_2. CO_2 concentrations were monitored daily by sterilely removing 100 μl gas samples which were analyzed by gas chromatography (GC) with a thermal conductivity detector (series 6890, Agilent Technologies, Santa Clara, CA, USA) and a GS-CarbonPLOT 30 m × 0.32 mm × 3.0 mm column, using argon as the carrier gas with a column flow rate of 1.6 ml min^{-1}. The oven temperature was 35°C and the detector temperature was 150°C. All bioreactor experiments were run in triplicate. Biomass, OD_{730}, and $\%CO_2$ measurements were taken daily over the course of each nine-day experiment. Prior to harvesting the cells, an aliquot was removed sterilely and cultured on BG-11 agar to screen for contamination.

Cellular CO_2 uptake rates calculated from the CO_2 fixation rate shown in Table 1 were several orders of magnitude lower than rates of gas-phased CO_2 transfer into the liquid (data not shown). In addition, Hill [17] showed that in a well-mixed reactor, the reaction rate of aqueous $CO_2 \leftrightarrows H_2CO_3$ was 100 times faster than the maximum mass transfer rate. Using carbonic acid concentration as a proxy for aqueous CO_2 concentrations, he observed a slight delay (100 s) in the accumulation of carbonic acid at the beginning of CO_2 addition and the attainment of equilibrium within 300 s. This is quite rapid compared to the rates

Table 1 Specific growth rates, productivity, CO_2 fixation rates, and percent CO_2 utilization of *T. elongatus* under increasing carbon concentrations

Inlet CO_2 concentration	Specific growth rate (day^{-1})	Productivity (mg ml^{-1} day^{-1})	CO_2 fixation rate (mg ml^{-1} day^{-1})	Percent CO_2 used (%)
Atmospheric	0.011 ± 0.04	0.01 ± 0.003	0.02 ± 0.009	54.54 ± 4.37
5%	0.11 ± 0.04	0.07 ± 0.02	0.14 ± 0.05	5.31 ± 0.00
10%	0.12 ± 0.01	0.07 ± 0.01	0.13 ± 0.02	1.70 ± 0.35
20%	0.13 ± 0.02	0.09 ± 0.01	0.17 ± 0.01	1.36 ± 0.17

Values are the average of three samples ± SD

of cellular CO_2 uptake and cell growth. Therefore, given these observations and that acid–base reactions in aqueous media are generally considered to occur instantaneously, it is reasonable to assume that the carbonate species (Table 2) were at equilibrium in the bioreactors and that headspace CO_2 measurements could be used as a reliable surrogate for aqueous carbonate species concentrations.

Biomass analysis

Biomass concentrations were measured gravimetrically by centrifuging the cells and drying the resultant cell pellets at 60°C for 24 h. Elemental analysis was done to determine total carbon and nitrogen using a Costech Instruments ECS 4010 system (Costec Analytical Technologies, Valencia, CA, USA). The biomass was dried and a <2 mg sample was oxidized at 1,000°C, and the resulting gases were measured and compared to an atropine standard. After removal of the cells, the carbon content of the supernatant was also measured by elemental analysis.

Carbon storage compounds

Lipids were extracted and quantified following the colorimetric method of Christie [7] modified from the method of Folch et al. [13]. Samples were dried, and then resuspended in 5 ml $CHCI_3$–MeOH (2:1 v/v) and incubated, shaking overnight at room temperature. Following centrifugation, the supernatant was saved and the pellet extracted twice more with 5 ml $CHCI_3$–MeOH (2:1 v/v). KCl was added to a final concentration of 0.88% to the combined supernatant volume, which was then mixed and centrifuged. An aliquot of the bottom fraction containing the lipids was then boiled for 45 min with potassium dichromate and the absorbance was measured at 350 nm. A standard curve was generated using palmitic acid. Total carbon in the lipid extracts was determined by elemental analysis.

Polyhydroxybutyrate extraction followed the method of Law and Slepecky, which uses heat and H_2SO_4 to quantitatively convert PHBs to crotonic acid [25]. PHBs were extracted by boiling the samples in chloroform at 60°C for 6 h. The samples were filtered through a glass filter while hot. A 0.5 ml aliquot was then evaporated, 4 ml H_2SO_4 were added, the sample was boiled at 100°C for 10 min, and the absorbance was measured at 230 nm. A standard curve was made by dissolving PHB granules (GoodFellow, Oakdale, PA, USA) in H_2SO_4.

Glycogen measurements were based on the extraction method of Ernst [12]. Cells were concentrated to an optical density of 600 µg Chl/ml in a final volume of 50 µl. Two hundred microliters of 30% (w/v) KOH were added and the samples were heated at 100°C for 90 min. The extracts were then cooled, 600 µl ethanol were added, and the samples were incubated on ice for 2 h. The glycogen was collected by centrifugation at 15,000×*g* for 5 min. The pellet was washed twice with ethanol and dried for 10 min at 60°C, and then resuspended in 300 µl 100 mM sodium acetate (pH 4.75). Following resuspension, 10 µl amyloglucosidase and 10 µl amylase were added, and the samples were incubated 1 h at room temperature to convert the glycogen to glucose. Insoluble fragments were removed by centrifuging at 1,500×*g* for 10 min, and the glucose in the supernatant was quantified using a glucose assay kit (product # GAGO20, Sigma-Aldrich, St. Louis, MO, USA). A glycogen standard was also used to ensure the enzymatic digest was complete during the incubation time and to correlate glucose concentration to the initial glycogen concentration.

Results

Growth and biomass analysis

Thermosynechococcus elongatus was able to grow on up to 20% CO_2 in the photobioreactors. At 30% CO_2, the cultures died and bleached out within 24 h. Cultures grown on 5–20% CO_2 showed similar growth characteristics to those measured by OD_{730} (Fig. 1). The growth rate for cultures grown at each CO_2 concentration was modeled using a zero-order kinetic model:

Table 2 Carbonate equilibrium species under increasing CO_2 concentrations at 50°C

CO_2 (%)	CO_2 in headspace (moles)	Aqueous CO_2 (mol/l)	H_2CO_3 (mol/l)	HCO_3 (mol/l)	CO_3^{2-} (mol/l)
Atmospheric	1.49×10^{-4}	6.73×10^{-6}	2.33×10^{-7}	2.15×10^{-4}	7.63×10^{-7}
5%	2.07×10^{-3}	9.35×10^{-4}	3.24×10^{-5}	2.99×10^{-2}	1.06×10^{-4}
10%	4.15×10^{-3}	1.87×10^{-3}	6.47×10^{-5}	5.97×10^{-2}	2.12×10^{-4}
20%	8.30×10^{-3}	3.74×10^{-3}	1.29×10^{-4}	1.19×10^{-1}	4.24×10^{-4}

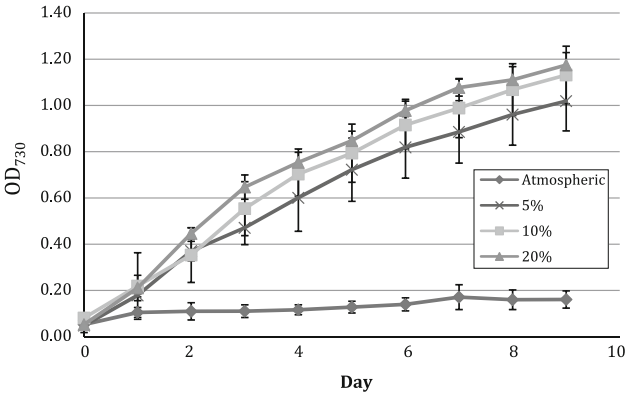

Fig. 1 Growth curves of *T. elongatus* with gas of increasing CO_2 concentrations bubbling. Cell density measured as the optical density at 730 nm. Data points represent the mean ($n = 3$). *Error bars* indicate the standard deviation from the mean

$$\frac{dX}{dt} = k. \tag{1}$$

k was estimated by fitting a line to the growth data. Cultures grown with atmospheric CO_2 showed very little growth and achieved a specific growth rate of only 0.011 day^{-1}, while a maximum specific zero-order growth rate of 0.13 day^{-1} was achieved with cells grown on 20% CO_2 (Table 1). Similar culture densities were achieved at 5–20% CO_2, while the maximum cell density under atmospheric CO_2 concentrations was at an OD_{730} of 0.16 (Fig. 1). The results of the total carbon and nitrogen analyses showed that the molar ratio of C:N did not change under the range of CO_2 concentrations tested, and remained approximately 5.2:1 (data not shown).

Biomass productivity as a function of substrate concentration was modeled using the Monod expression for the net rate of cell growth:

$$r_{\text{net}} = Y\frac{V_{\max}S}{K_s + S}X - bX, \tag{2}$$

where r_{net} is the net rate of cell growth (mg ml^{-1} day^{-1}), which is equal to the productivity, $V_{\max}$ is the maximum specific first-order substrate utilization rate (mg ml^{-1} day^{-1}), K_s is the half-saturation coefficient (%), and S is the gas phase substrate concentration (%). Gas phase concentrations were used as surrogates for the liquid phase concentrations since they could be measured directly and gas–liquid phase equilibrium is achieved rapidly relative to the cellular CO_2 uptake rates that were observed [17]. X is the concentration of active biomass (mg/l), and b is the endogenous decay coefficient (day^{-1}). The initial fit to the model was the same whether or not the endogenous decay coefficient was included. Also, the maximum specific zero-order growth rate ($\mu_{\max}$) was substituted for $YV_{\max}$, thus simplifying Eq. 2 as follows (defined in terms of the productivity P):

$$P = \frac{\mu_{\max}S}{K_s + S}. \tag{3}$$

K_s and $\mu_{\max}$ were determined by nonlinear regression and by minimizing the sum. The best-fit estimate of K_s was 1.37% and $\mu_{\max}$ was estimated at 0.09 mg ml^{-1} day^{-1}. The results of the model are shown in Fig. 2. Productivity increased as the CO_2 concentration increased from atmospheric to 5%. From 5 to 20% there was no statistically significant increase in biomass productivity (Table 1).

Maximum biomass productivity of *T. elongatus* was 0.09 ± 0.01 mg ml^{-1} day^{-1} with 20% CO_2 while the productivity was only 0.01 ± 0.003 mg ml^{-1} day^{-1} at atmospheric CO_2 (Table 1). CO_2 fixation rates were calculated using the following equation from Wang et al. [44]:

$$P_{(CO_2)} = 1.88 \times P, \tag{4}$$

where P is the biomass productivity (mg ml^{-1} day^{-1}) and $P_{(CO_2)}$ is the CO_2 fixation rate (mg ml^{-1} day^{-1}). This equation is derived from the molecular formula for microalgae biomass, $CO_{0.48}H_{1.83}N_{0.11}P_{0.01}$ [6], and has also been applied to cyanobacteria [44]. CO_2 uptake rate calculations using this method were compared to the method of Kajiwara et al. [22], which incorporates the measured biomass carbon content, and the results were found to be virtually identical. CO_2 fixation rates reached a maximum of 0.17 ± 0.01 mg ml^{-1} day^{-1} at 20% CO_2 (Table 1). The percent CO_2 utilization was calculated by dividing the amount of CO_2 fixed per day by the CO_2 feed rate per day. The percent CO_2 utilization decreased with increasing CO_2 concentration. With no supplemental CO_2 (atmospheric concentrations), 54.5 ± 4.4% of the total CO_2 was used. The percent used decreased with increasing CO_2 concentrations and reached a minimum of 1.4 ± 0.2% with an inlet CO_2 concentration of 20% (Table 1). The maximum

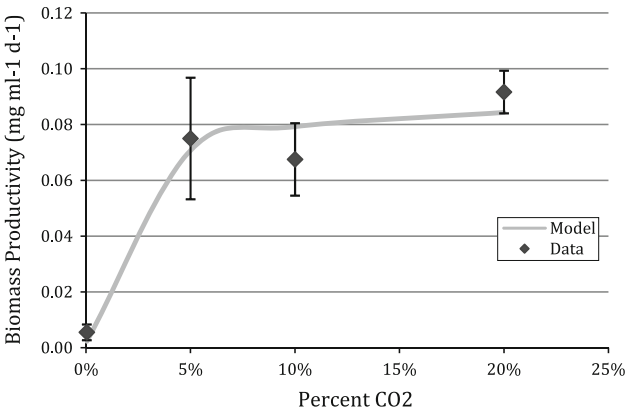

Fig. 2 Monod model of maximum biomass accumulation with increasing concentrations of CO_2. Data points represent the mean ($n = 3$). *Error bars* indicate the standard deviation from the mean

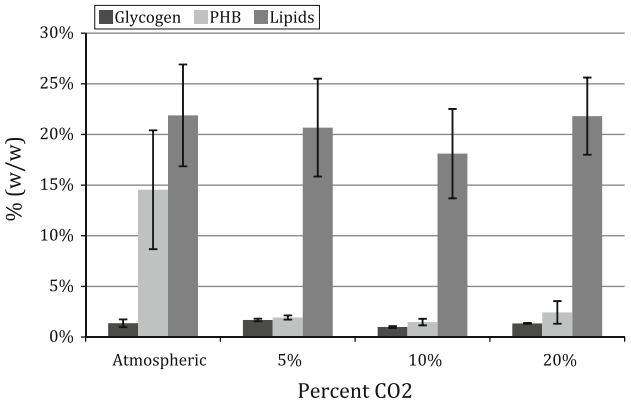

Fig. 3 Glycogen, lipid, and PHB contents in *T. elongatus* grown over a range of 0–20% CO_2. Data points represent the mean ($n = 3$). *Error bars* indicate the standard deviation from the mean

amount of CO_2 sequestered over the course of the nine-day bioreactor experiment was 1.15 g l^{-1} in cultures grown on 20% CO_2. The maximum photosynthetic efficiency of CO_2 fixation was around 7.98% of the theoretical maximum at a light intensity of 180 μE m^{-2} s^{-1}. This calculation was based on 48% of the total light being photosynthetically active radiation and the requirement of eight photons to fix one molecule of CO_2 [41].

Henry's law was used to determine the solubility of CO_2 in the media under the experimental CO_2 concentrations using the following equation:

$$x_g = \frac{P_T}{H}\rho_g, \tag{5}$$

where x_g is the mole fraction of gas in water (mole gas/mole water), P_T is the total pressure (1 atm), H is Henry's constant (atm) adjusted for temperature, and ρ_g is the mole fraction of gas in air (moles gas/moles air). Henry's constant at 50°C is 2971 atm [30]. The mole fraction was then converted to moles of gas per liter of water by multiplying by the formula weight (g/mole) and the density of water (g/l). The headspace molar concentration of CO_2 was calculated using the ideal gas law. The solubility of CO_2 was calculated at 30 and 50°C, and the aqueous CO_2 concentration was found to be 38% lower at 50°C. Based on carbonate system equilibrium at pH 7.8, the concentration of HCO_3^- was 0.215 mM with no supplemental CO_2 addition, 30 mM at 5% CO_2, 60 mM at 10% CO_2, and 120 mM at 20% CO_2.

Carbon storage compounds

The concentration of lipids did not vary significantly over the range of test conditions studied in these experiments. The average lipid content was approximately 20.0% (w/w) in all samples (Fig. 3). In contrast, the PHB content varied significantly. Cultures that were not given supplemental CO_2 contained about 14.5% (w/w) PHB, while cultures that had 5–20% CO_2 accumulated only about 2.0% PHB (Fig. 3). No clear trend could be seen between CO_2 concentration and glycogen content, which remained low [about 1.4% (w/w)] under all test conditions (Fig. 3).

The amount of carbon in each storage compound was also determined. Lipids averaged 75.6 ± 1.4% carbon by weight based on elemental analysis. Both PHB and glycogen are polymeric compounds. The percentage of carbon in these compounds on a molar basis was used to calculate the total mass of carbon they contained. Lipids, PHBs, and glycogen accounted for approximately 50% of the total carbon in cells grown on atmospheric CO_2. At 5–20% CO_2 they only accounted for about 30% of the total carbon in the biomass (Fig. 4). Total carbon accounted for around 48% of the total cell dry weight under all test conditions (Fig. 4). The amount of carbon remaining in the supernatant after harvesting the cells was also measured but did not vary significantly between 5 and 20% CO_2. However, in

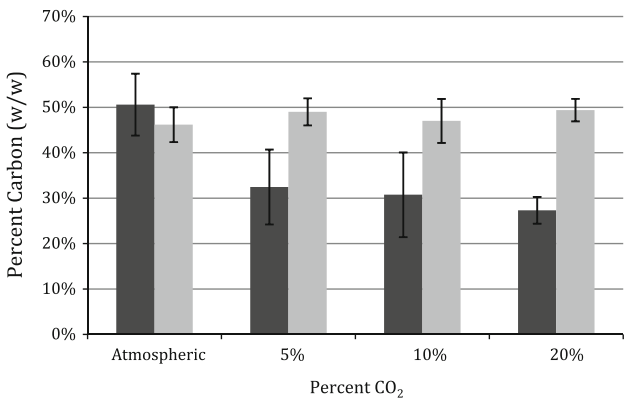

Fig. 4 *Dark bars*: percent of total carbon in lipids, PHBs, and glycogen. *Light bars*: total carbon content as a percent of cell dry weight. Data points represent the mean ($n = 3$). *Error bars* indicate the standard deviation from the mean

cultures grown on atmospheric CO_2 concentrations, there was only about 40% as much carbon present in the media (data not shown).

Discussion

Growth of cyanobacteria on high levels of CO_2 has been described in many mesophilic species [31, 37, 44]; however, much less is known about the response of thermophilic strains. Recently, the growth of the thermophilic cyanobacterium *Thermosynechococcus* sp. CL-1 was described on 10 and 20% CO_2 [19]. Saki et al. [40] noted at the time of their work with a thermophilic strain of *Chlorella* that there were very few reports in the literature regarding CO_2 tolerance in thermophilic organisms. Now, 15 years later, little has changed in that regard. However, several recent reviews have recognized the need for this subject to be addressed, especially in regard to the operation of bioreactors [24, 29]. In addition, data are scarce on the growth and kinetic parameters of CO_2 uptake in thermophilic cyanobacteria.

In *T. elongatus*, differences in biomass accumulation rates were not statistically significant between 5 and 20% CO_2, indicating that even though the cells can tolerate higher levels, their ability to take up CO_2 were saturated at 5% or less under the conditions of these experiments (Table 1). Growth, productivity, and carbon assimilation rates observed in *T. elongatus* compared favorably with those of other thermophilic cyanobacteria. Ono and Cuello [36] found that *Chlorogleopsis* sp. reached a maximum carbon assimilation rate of 0.02054 mg ml^{-1} day^{-1} with 5% CO_2. In contrast, *T. elongatus* was able to achieve a carbon fixation rate that was eight times higher with 20% CO_2 (Table 1). However, the maximum biomass concentration was only 0.833 mg ml^{-1} with 20% CO_2 (Table 1), compared to 1.24 mg ml^{-1} in *Chlorogleopsis* sp. [36]. The lower total biomass may be due in part to shorter culturing times, which were only 9 days compared to 28 days for *Chlorogleopsis* sp., or to light limitation caused by self-shading in the bioreactors.

In contrast, several mesophilic species are capable of growth on high levels of CO_2 with higher productivity. Recent work with *Spirulina* sp. found a maximum specific growth rate of 0.44 day^{-1}, a productivity of 0.22 mg ml^{-1} day^{-1}, a maximum biomass concentration of 3.50 mg ml^{-1}, and a CO_2 fixation rate of 0.413 mg ml^{-1} day^{-1} when grown on 6 and 12% CO_2 [8]. The specific growth rate of *Spirulina* sp. was similar to *T. elongatus* grown on 20% CO_2, but productivity and CO_2 fixation rates were over twice as high. Even higher CO_2 fixation rates of up to 1.5 mg ml^{-1} day^{-1} have been achieved with *Synechocystis aquatilis* [34]. The higher CO_2 fixation rates of mesophiles may be due in part to the higher solubility of CO_2 at lower temperatures. At 30°C, the soluble concentration of CO_2 is 38% greater than at 50°C for any given headspace CO_2 concentration. Therefore, the available CO_2 in solution is significantly higher, leading to potentially higher uptake rates.

Up to 54.5 ± 4.4% of the CO_2 was utilized by *T. elongatus* when grown with no CO_2 supplementation. The efficiency of CO_2 utilization decreased at higher concentrations, reaching a minimum value of 1.3 ± 0.17% at 20% CO_2 (Table 1). The amount of CO_2 utilized at 10–20% was similar to reports for other species. Jacob-Lopes et al. [20] found that *Aphanothece microscopica Nägeli* was able to utilize a maximum of 3.1 ± 0.05% with 15% CO_2.

The amount of carbon remaining in the supernatant after harvesting the cells did not vary significantly between 5 and 20% CO_2, indicating that the carbonate equilibrium species were not a significant contributor to the carbon content of the media. In addition, cultures grown on atmospheric carbon concentrations had significantly less carbon in the media. This suggests that a significant amount of the carbon not used in growth or storage compounds was excreted. Cyanobacteria are known to produce large amounts of secondary metabolites such as exopolysaccharides (EPS) [1]. Although total protein was not measured, the total biomass carbon as a percentage of cell dry weight was around 48% under all test conditions (Fig. 4), indicating that the content of other cellular components, such as proteins, was significantly less under atmospheric CO_2 concentrations.

Very little data are available on the lipid contents of thermophilic cyanobacteria. One exception is *Thermosynechococcus* sp. CL-1, which was reported to contain around 13% (w/w) when grown on 10% CO_2 [19]. This is significantly less than the 20% (w/w) lipid content found in *T. elongatus*.

The percentage of total biomass carbon in lipids, PHBs, and glycogen was significantly higher in cultures that were grown without supplemental CO_2 (Fig. 3). This was primarily due to the concentration of PHBs, which was seven times higher without supplemental CO_2, perhaps due to stress induced by carbon limitation. PHB accumulation is a known stress response under nutrient deprivation. For example, studies of the thermophilic cyanobacterium *Synechococcus* sp. MA19 have shown PHB accumulation to levels of up to 27% (w/w) under nitrogen-depleted conditions [32], and it appears that carbon limitation may cause a similar stress response in *T. elongatus*. PHB levels in *T. elongatus* grown on atmospheric CO_2 levels were comparable to those of *Synechococcus* sp. MA19, which has been reported to store up to 20% dry weight using CO_2 as its sole carbon source [32].

The PHB content generally appears to be lower in mesophilic cyanobacteria. In *Synechocystis* PCC 6803,

PHB concentrations of 7% dry weight have been reported in wild-type cells, with mutant strains producing up to 11% dry weight [43]. PHB production has also been studied extensively in several *Spirulina* strains. Reports of PHB concentrations in *Spirulina maxima* vary from 0.1 to 6%, depending on the conditions [3, 9]. The PHB levels were also similar to *T. elongatus* grown in 150 ml shaking flask experiments on 5–150 mM initial dissolved organic carbon (DIC) concentrations. Previous work in our lab has shown that at low levels of DIC (5 mM), cultures accumulated over 10% (w/w) PHB, which decreased to around 2% (w/w) in cultures grown on 60–150 mM DIC (data not shown).

Glycogen levels averaged approximately 13.5 mg g^{-1} dry cell weight, which is similar to the glycogen level of 10.5 mg g^{-1} reported for *Synechocystis* sp. PCC 6803 [45]. However, when incubated under nitrogen-deprived conditions, glycogen levels in *Synechocystis* sp. PCC 6803 can be as much as three times higher than when grown in a nitrogen-rich environment [45]. Currently it is unknown if *T. elongatus* would produce higher glycogen levels under nitrogen-deprived conditions.

The consistency of glycogen production at all CO_2 levels is somewhat surprising (Fig. 3). Previous work in our lab demonstrated that the concentration of DIC had a significant effect on the amount of glycogen produced by *T. elongatus*. Cultures grown at 5–60 mM DIC accumulated around 2.5% (w/w) glycogen, while the concentration increased to around 8% (w/w) at 100 mM DIC, and reached 15% (w/w) at 150 mM glycogen content (data not shown). The reason for this difference is not clear, especially since at 20% CO_2 and pH 7.8 the effective bicarbonate concentration based on carbonate equilibrium calculations is around 120 mM. Therefore, it would seem likely that, unless the cells behave quite differently in a bioreactor, the amount of glycogen accumulated should be nearly the same as in cultures grown on 100–150 mM DIC in batch cultures.

Cultures grown on CO_2 in the bioreactors may have been light limited. Although the light intensity was much higher than in the DIC experiments, the bioreactor design was such that they could only be illuminated from below, leading to self-shading at high cell densities. The cultures grown on DIC may have had excess energy that could be diverted to sequestering carbon while they were in a carbon-rich environment. In contrast, cultures grown on CO_2 may have only received enough light to maintain growth, with no extra energy available to build up carbon reserves.

The possibility of different carbon uptake mechanisms being activated when grown on CO_2 merits further investigation. *T. elongatus* has homologous sequences for *cmpABCD*, an inducible high-affinity HCO_3^- ATP-dependent transporter; for *ndhF3*, which is involved in inducible high-affinity CO_2 transport; and for *ndhF4*, which is involved in low-affinity CO_2 transport. However, it has no homologs to the low-affinity Na^+-dependent HCO_3^- symporter *sbtA* gene [4]. Due to the apparent absence of a low-affinity, constitutively expressed HCO_3^- transporter, it is difficult to explain why *T. elongatus* can grow so well and store so much glycogen when grown on high levels of HCO_3^-.

A specialized NDH-1 complex has also been postulated as a mechanism for converting CO_2 to HCO_3^- in cyanobacteria. The proposed system is thought to couple the hydration of CO_2^- with photosynthetic electron transport and the translocation of protons across the thylakoid membrane [4]. Such a system would place an additional energy demand on the cell, further limiting glycogen synthesis.

One key issue that this study did not address is the effect of the diurnal cycle on CO_2 sequestration and biomass productivity. Since CO_2 fixation only occurs during daylight, actual productivity and sequestration rates in outdoor bioreactors will be lower. As a result, in considering industrial CO_2 sequestration, nighttime emissions will not be captured. Other methods would need to be used to temporarily sequester CO_2 as a carbonate species at night, which could then be utilized by cyanobacteria during the day.

Acknowledgments We would like to thank Dr. Elizabeth Burrows for her technical assistance in setting up and troubleshooting the bioreactors. This work was supported in part by the DOD/ASEE SMART scholarship program. Special thanks to Markael Luterra for editorial assistance.

References

1. Abed R, Dobretsov S (2009) Applications of cyanobacteria in biotechnology. J Appl Microbiol 106:1–12
2. Antoni D, Zverlov VV, Schwarz WH (2007) Biofuels from microbes. Appl Microbiol Biotechnol 77(1):23–35
3. Asada Y, Miyake M, Miyake J, Kurane R, Tokiwa Y (1999) Photosynthetic accumulation of poly-(hydroxybutyrate) by cyanobacteria—the metabolism and potential for CO_2 recycling. Int J Biol Macromol 25:37–42
4. Badger M, Price G (2003) CO_2 concentrating mechanisms in cyanobacteria: molecular components, their diversity and evolution. J Exp Bot 54(383):609–622
5. Castenholz RW (1988) Thermophilic cyanobacteria: special problems. Method Enzymol 167:96–100
6. Chisti Y (2007) Biodiesel from microalgae. Biotechnol Adv 25(3):294–306
7. Christie W (1973) Lipid analysis: isolation, separation, identification, and structural analysis of lipids. Pergamon, Oxford
8. de Morais M, Costa J (2007) Biofixation of carbon dioxide by *Spirulina* sp. and *Scenedesmus obliquus* cultivated in a three-stage serial tubular photobioreactor. J Biotechnol 129:439–445
9. De Philippis R, Sili C, Vincenzini M (1992) Glycogen and poly-{beta}-hydroxybutyrate synthesis in spirulina maxima. Microbiology 138:1623–1628
10. Diamond L, Akinfiev N (2003) Solubility of CO_2 in water from −1.5 to 100 °C and from 0.1 to 100 MPa: evaluation of literature

data and thermodynamic modelling. Fluid Phase Equilib 208(1–2):265–290
11. Eckert JS, Foote EH, Rollison LR, Walter LF (1967) Absorption processes utilizing packed towers. Ind Eng Chem 59(2):41–47
12. Ernst A, Kirschenlohr H, Diez J, Böger P (1984) Glycogen content and nitrogenase activity in anabaena variabilis. Arch Microbiol 140(2–3):120–125
13. Folch J, Lees M, Stanley G (1957) A simple method for the isolation and purification of total lipides from animal tissues. J Biol Chem 226(1):497
14. Gill NK, Appleton M, Baganz F, Lye GJ (2008) Quantification of power consumption and oxygen transfer characteristics of a stirred miniature bioreactor for predictive fermentation scale-up. Biotechnol Bioeng 100(6):1144–1155
15. Hai T, Oppermann-Sanio F (1999) Purification and characterization of cyanophycin and cyanophycin synthetase from the thermophilic *Synechococcus* sp. Ma19. FEMS Microbiol Lett 181:229–236
16. Harun R, Singh M, Forde G, Danquah M (2010) Bioprocess engineering of microalgae to produce a variety of consumer products. Renew Sustain Energy Rev 14(3):1037–1047
17. Hill GA (2006) Measurement of overall volumetric mass transfer coefficients for carbon dioxide in a well-mixed reactor using a pH probe. Ind Eng Chem Res 45(16):5796–5800
18. Holladay J, White J, Bozell J, Johnson D (2007) Top value-added chemicals from biomass. Volume 2—results of screening for potential candidates from biorefinery lignin. Pacific Northwest National Laboratory, Richland
19. Hsueh H, Li W, Chen H, Chu H (2009) Carbon bio-fixation by photosynthesis of *Thermosynechococcus* sp. Cl-1 and *Nannochloropsis oculta*. J Photochem Photobiol B 95:33–39
20. Jacob-Lopes E, Gimenes Scoparo C (2010) Biotransformations of carbon dioxide in photobioreactors. Energy Convers Manag 51:894–900
21. Jordan P, Fromme P, Witt HT, Klukas O, Saenger W, Krauss N (2001) Three-dimensional structure of cyanobacterial photosystem I at 2.5 Å resolution. Nature 411(6840):909–917
22. Kajiwara S, Yamada H, Ohkuni N (1997) Design of the bioreactor for carbon dioxide fixation by *Synechococcus* PCC7942. Energy Convers Manag 38:S529–S532
23. Kromkamp J (1987) Formation and functional significance of storage products in cyanobacteria. NZ J Mar Freshw Res 21:457–465
24. Kunjapur A, Eldridge R (2010) Photobioreactor design for commercial biofuel production from microalgae. Ind Eng Chem Res 49:3516–3526
25. Law J, Slepecky R (1961) Assay of poly-b-hydroxybutyric acid. J Bacteriol 82(1):33–36
26. Li Y, Horsman M, Wu N, Lan C, Dubois-Calero N (2008) Biofuels from microalgae. Biotechnol Prog 24(4):815–820
27. Loll B, Kern J, Saenger W, Zouni A, Biesiadka J (2005) Towards complete cofactor arrangement in the 3.0 Å resolution structure of photosystem II. Nature 438(7070):1040–1044
28. Mallick N (2002) Biotechnological potential of immobilized algae for wastewater N, P and metal removal: a review. Biometals 15:377–390
29. Mata T, Martins A, Caetano N (2010) Microalgae for biodiesel production and other applications: a review. Renew Sustain Energy Rev 14:217–232
30. Metcalf E, Tchobanoglous G, Burton FL, Stensel HD (2004) Wastewater engineering: treatment and reuse (McGraw-Hill Series on Civil and Environmental Engineering), 4th edn. McGraw-Hill, Boston
31. Miyachi S, Iwasaki I, Shiraiwa Y (2003) Historical perspective on microalgal and cyanobacterial acclimation to low- and extremely high-CO_2 conditions. Photosynth Res 77:139–153
32. Miyake M, Erata M, Asada Y (1996) A thermophilic cyanobacterium, *Synechococcus* sp. Ma19, capable of accumulating poly-[beta]-hydroxybutyrate. J Ferment Bioeng 82(5):512–514
33. Miyake M, Takase K, Narato M, Khatipov E, Schnackenberg J, Shirai M, Kurane R, Asada Y (2000) Polyhydroxybutyrate production from carbon dioxide by cyanobacteria. Appl Biochem Biotechnol 84–86:991–1002
34. Murakami M, Ikenouchi M (1997) The biological CO_2 fixation and utilization project by RITE (2)—screening and breeding of microalgae with high capability in fixing CO_2. Energy Convers Manag 38:S493–S497
35. Nakamura Y, Kaneko T, Sato S, Ikeuchi M, Katoh H, Sasamoto S, Watanabe A, Iriguchi M, Kawashima K, Kimura T, Kishida Y, Kiyokawa C, Kohara M, Matsumoto M, Matsuno A, Nakazaki N, Shimpo S, Sugimoto M, Takeuchi C, Yamada M, Tabata S (2002) Complete genome structure of the thermophilic cyanobacterium *Thermosynechococcus elongatus* BP-1 (supplement). DNA Res 9(4):135–148
36. Ono E, Cuello J (2007) Carbon dioxide mitigation using thermophilic cyanobacteria. Biosyst Eng 96(1):129–134
37. Papazi A, Makridis P, Divanach P (2008) Bioenergetic changes in the microalgal photosynthetic apparatus by extremely high CO_2 concentrations induce an intense biomass production. Physiol Plant 132:338–349
38. Porra R (2002) The chequered history of the development and use of simultaneous equations for the accurate determination of chlorophylls a and b. Photosynth Res 73(1):149–156
39. Van't Reit K (1979) Review of measuring methods and results in nonviscous gas–liquid mass transfer in stirred vessels. Ind Eng Chem Process Des Dev 18(3):357–364
40. Sakai N, Sakamoto Y, Kishimoto N, Chihara M (1995) *Chlorella* strains from hot springs tolerant to high temperature and high CO_2. Energy Convers Manag 36(6–9):693–696
41. Scott S, Davey M, Dennis J, Horst I (2010) Biodiesel from algae: challenges and prospects. Curr Opin Biotechnol 21:277–286
42. Singh J, Gu S (2010) Commercialization potential of microalgae for biofuels production. Renew Sustain Energy Rev 14:2596–2610
43. Sudesh K, Iwata T (2008) Sustainability of biobased and biodegradable plastics. Clean 36(5–6):433–442
44. Wang B, Li Y, Wu N, Lan C (2008) CO_2 bio-mitigation using microalgae. Appl Microbiol Biotechnol 79:707–718
45. Yoo S, Keppel C, Spalding M, Jane J (2007) Effects of growth condition on the structure of glycogen produced in cyanobacterium *Synechocystis* sp. Pcc6803. Int J Biol Macromol 40:498–504